COBEM 2021 26th International Congress of Mechanical Engineering
ABCM Associação Brasileira de Engenharia e Ciências Mecânicas
November 22-26, 2021, Virtual Congress, Brazil

COB-2021-2006 THE DESTRUCTIVE POWER OF UNBALANCE ON ROTATING MACHINES - CASE STUDY AND EXPERIMENTAL APPLICATIONS

Marcelo dos Reis Farias
Centro Federal de Educação Tecnológica Celso Suckow da Fonseca (CEFET) – R. do Areal, 522 - Parque Perequê, Angra dos Reis - RJ, 23953-030. / Universidade Federal do Rio de Janeiro (UFRJ), Programa de Engenharia Oceânica - Av. Athos da Silveira Ramos - Cidade Universitária, Rio de Janeiro, Brasil - 21941-611
marcelo.farias@cefet-rj.br

Paulo Victor Gomes dos Santos
Centro Federal de Educação Tecnológica Celso Suckow da Fonseca (CEFET) – R. do Areal, 522 - Parque Perequê, Angra dos Reis – Rio de Janeiro, Brasil - 23953-030.
paulo.gomes@cefet-rj.br

Paulo Roberto Farias Junior
Centro Federal de Educação Tecnológica Celso Suckow da Fonseca (CEFET) – Estr. de Adrianópolis, 1317 - Vila Nossa Sra. da Conceicao, Nova Iguaçu - RJ, 26041-271 / Departamento de Engenharia Mecânica (PGMEC-TEM), Universidade Federal Fluminense, UFF, Rua Passo da Pátria, 156, Bloco E, Sala 210, Niterói, RJ CEP, 24210-240, Brasil
paulo.farias@cefet-rj.br

Abstract. *In order to meet the global requirements of growing demand for fast production and the increase of quality, the industries need to keep their assets operational for as long as possible, then needing a maintenance plan suitable for their objectives. In industrial processes, a large part of the assets and machinery is composed of rotating machines, which, among various possibilities of defects and malfunctions, must always be properly balanced so that they can operate properly. This article presents the destructive power of unbalancing in rotating machines through a case study of a large exhaust system, where unbalance was diagnosed and fixed by using vibratory behavior monitoring. The theoretical concepts about the unbalance in this case study are presented in an analytical way and applied through a simulation using Kane's method, and also using experiments in a laboratory test bench. The results show that through the vibration analysis it is possible to monitor unbalance in rotating machines, increasing the reliability of the industrial plant and preventing failures, which causes economic losses and can also cause damage to the human health of workers exposed to an unbalanced machine. The simulations and laboratory experiments are good tools for a better understanding of the unbalance effects on the machine.*
Keywords: *vibration, maintenance, unbalance, balancing.*

1. INTRODUCTION

1.1 Unbalance concepts

The unbalance of shafts and rotors in rotating machines can be seen as one of the main problems found in industrial maintenance. Research conducted by the International Maintenance Conference IMC-2012 released by the site reliability web Levitt (2021) evaluating maintenance professionals pointed out the unbalance as the third type of defect that is most frequently found by predictive inspectors in rotating machines, where first is the misalignment and second is bearing defect. According to a technical article published in 2019 by Braga (2019), unbalance is the fault that most causes vibrations in rotating machines.

Unbalance is characterized by the difference between the center of rotation and the center of mass of a system. That is, when in a rotating system we have a heavier (or lighter) point displaced from the center of rotation, we have an unbalanced condition. Agnieszka Muszynska in her book "Rotordynamics" treats the rotor unbalance as a condition of unequal mass distribution in the radial direction at each axial section of the rotor system; thus, in an unbalanced condition, the rotor mass centerline does not coincide with the axis of rotation. The "heavy spot" is a term often used in machinery rotors to refer to unbalance, which means the angular location, at the rotor lateral cross-section, where the unbalance is situated Muszynska (2005).

In rotating machines, one of the most direct ways to perceive, identify and monitor an unbalance is through mechanical vibrations. The greater the level of unbalancing, the greater the tendency to increase the vibration level of a machine. In

the case of a rotating system, one of the biggest villains and influencers of these vibrations due to unbalance is the rotation speed, as the unbalance force is proportional to the square of the angular velocity of the system Rao (2009). In this way, the greater the angular velocity of an unbalanced system, the greater the harmonic force exerted on it, and, consequently, it will tend to have a greater range of motion (expressed through vibration), which can cause failures in components and structures, sometimes generating, catastrophic accidents.

It is worth noting that the unbalance will not always be undesired. There are applications where unbalance is used to purposely generate vibrations, as in the case of compaction machines, systems that use vibration to express sensitivity (video game controls), mechanical vibration excitation systems, massage equipment, fatigue testing machines by traction and compression efforts, among others.

However, when we talk about the most industrial rotating machines like pumps, motors, exhausts, turbines, etc; the unbalance will be unwanted, so the lower its level, the better the functioning of the machine in question. A correctly balanced machine will have a low vibration level, low energy consumption, low noise level, and less mechanical stress on its components. On the other hand, an unbalanced machine will present the opposite symptoms to those mentioned, which may lead to failures in its components and even lead to a catastrophic accident reaching people. In fact, unbalance, linked to its vibration effect, has high destructive power. The amplification of vibratory movements generates overloads on the components, increase in temperature, increase in structural stresses and wear between rotating and fixed parts.

1.2 Unbalance Types

When a machine is unbalanced, the axis of rotor rotation is not coincident with its main axis of inertia and the position of how this axis is arranged in relation to the main axis of inertia determines the type of unbalance that the machine is suffering.

In static unbalance, the axis of rotation and the main axis of inertia are parallel, but not coincident and the force on the bearings are equal, parallel and in the same direction due to this arrangement of the axes Figure 1 a. In conjugate unbalance, the main axis of inertia is not parallel to the axis of rotation, but they intersect at the center of gravity of the rotor and the bearing loads are parallel, with the same intensity but with opposite directions Figure 1b . The dynamic case occurs when the axis of rotation is not parallel to the axis of the center of inertia and does not intersect at the center of gravity. This last type of unbalance is a combination of the two previous ones and the bearing loads are different in direction and intensity Figure 1 c Mobius (2005).

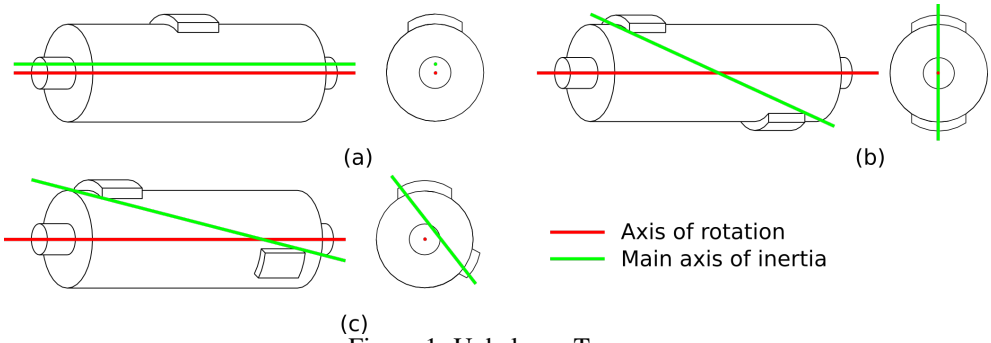

Figure 1: Unbalance Types.

1.3 Unbalance Causes and Symptoms

Even after having been balanced during commissioning or at the factory, there are some reasons why the machine can be unbalanced during its use, such as: Excessive dirt accumulated in the rotors unevenly; lack of homogeneity of materials, especially in castings; different dimensions of joining pieces (bolts, holes, keys); cracked rotors, roller deflection (rollers of paper machines), irregular corrosion or erosion of rotors; lost balance masses, water ingress in parts of the rotating system, among other numerous causes that generate the system's unbalanced.

If a machine is out of balance, one of the first symptoms to appear is a noticeable increase in vibration, often increasing the noise level as well. Another characteristic of an unbalanced system is the possible increase in bearing temperature due to high loads. Therefore, it is recommended to always have reference measurements of these parameters with the machine in good operating condition, so that inspection results can be compared not only with reference standards but with the machine's own history.

In the investigation of a possible case of unbalance, it is expected to observe in the time domain vibration graph a sine waveform with the frequency of the machine operating angular speed (1x Rpm) and in the frequency spectrum a high and dominant peak in the same frequency. Any rotor will always have some residual unbalance. Then, it must be determined when this level of unbalance will represent a problem, based on the amplitude levels through standards. For

a simply supported rotor, static unbalance will cause forces that reflect first order frequency shifts in both rotor support bearings, and the shifts in the horizontal direction of each bearing will occur in phase. In the case of conjugate unbalance, the centrifugal forces on the bearings will appear in phase opposition (180º). In dynamic unbalance, on the other hand, centrifugal forces will appear with an offset between 0° and 180° Mobius (2005).

1.4 Balancing Types

As noted by AHRI (2019), the rotor balancing procedure can be done in two general types called: static or dynamic rotor balancing. The method chosen is dependent upon many factors such as physical size, shape, rpm, mass, and unbalance limit requirements, which should be evaluated according to a standard rule reference as the ISO 21940.

Dynamic balancing would usually be employed if a rotor is relatively wide, compared to its diameter (width to diameter ratio is greater than 0.30) so that measurements and adjustments can be made in two axially separated correction planes. Static balancing, however, would be employed on a narrow rotor, where measurements and adjustments can be made in only one correction plane. It is important to note that, static balancing can be accomplished by either rotating or non-rotating means while dynamic balancing can only be accomplished by rotating means.

Non-rotating is the simplest method of static balancing that consists of a rotor mounted with its axis horizontal and allowed to pivot about its Shaft Axis. Any deviation of the center of mass relative to the Shaft Axis will cause it to pivot. Mass can then be added to or subtracted from the Rotor until there is no pivoting.

Dynamic balancing is normally accomplished with an electronic balancing machine which usually has a rotating horizontal arbor, with either hard or soft bearings, capable of measuring the amount and location of unbalance in each of two axially separated planes. The narrow width of propeller fans and narrow impellers make plane separation impractical, and corrections are only made in one plane. When an impeller is balanced dynamically, corrections are made in each of two correctional planes. This compensates for the "couple" effect caused when the unbalance locations for each plane are out of phase with each other. Correcting for unbalance is accomplished by adding or removing an appropriate amount of mass from one or more locations on an impeller/rotor.

1.5 Unbalance Diagnosis and Limits

Despite being a widespread subject in the industry and well studied and structured in the literature, predictive maintainers and inspectors still face some challenges in identifying and diagnosing unbalance in rotating machines because their characteristics (symptoms) are very similar to other types of defects. Therefore, when there is no periodic monitoring of the machine's condition, it is often difficult to diagnose the unbalance because it does not have a reference of the healthy machine behavior and sometimes cannot perform some specific evidential tests.

However, there are some standards that set limits on vibration or residual unbalance for different types and classes of rotating machines. Examples of these standards are: ISO 21940:2016, ISO 14694, NBR 15230, BS6861, ISO 6103, AMCA 204-05 e NBR8008. The standard ISO 21940 called as Mechanical vibration – Rotor balancing is one of the most used worldwide in industries and presents reference tables for residual unbalance limit values. Because of a wide range of variables involved in applying a component to a system, including a poorly designed system, the vibrational effect of the residual unbalance cannot be predicted unless all the system variables are considered AHRI (2019).

In recent years, with the increase of the machine amount and data from condition monitoring of machines, the data evaluation, and faults diagnosis procedures performed only by people are not adequately satisfying the global demand, and the intelligent data-driven approaches are emerging to offer promising tools for accurate machine condition assessment. Recent studies from Ramakrishnan Ambur and Stephan Rinderknecht Ambur and Rinderknecht (2018) unbalance faults were detected in the frequency domain using parameter estimation method. In the paper from Li *et al.* (2020) a novel method called "ACWGAN-GP" is proposed, which amplifies the capacity of generating new samples with high quality utilizing an unbalanced training set, and the generated samples have an excellent performance in unbalanced fault diagnosis of bearings and gearbox.

In the next topic of this article, we briefly present the theoretical foundations about unbalancing and its equation through Kane's method Kane and Levinson (1985). Next, we present a case study of a medium-sized industrial exhaust fan, used in a tire factory of a multinational company, which operated for some time unbalanced, generating large economic losses due to machine unavailability and initially inadequate maintenance. After correct identification of the problem (unbalance) and correction of it, the machine obtained 80% reduction in vibration levels and operated properly. Computational modeling using Kane's method was carried out with the data from the case study, and the results obtained in terms of computational simulation are compared with those observed in the real case. Then we use an experimental bench making an analogy with the real case to carry out tests to show, in a practical way, some primordial conclusions about the unbalance in rotating machines.

2. FUNDAMENTALS OF UNBALANCE THEORY

In this section a case of an unbalanced rotor, showed in Figure 2, is analyzed using Kane's method, Kane and Levinson (1985). In Figure 2, P designates an unbalanced mass that is fixed on the rotor B. The rotor B is rigidly clamped on the rigid shaft. The rigid shaft is supported by ball bearings. The stiffness of the ball bearing will be modeled as linear springs and the energy dissipation will be modeled as viscous damping.

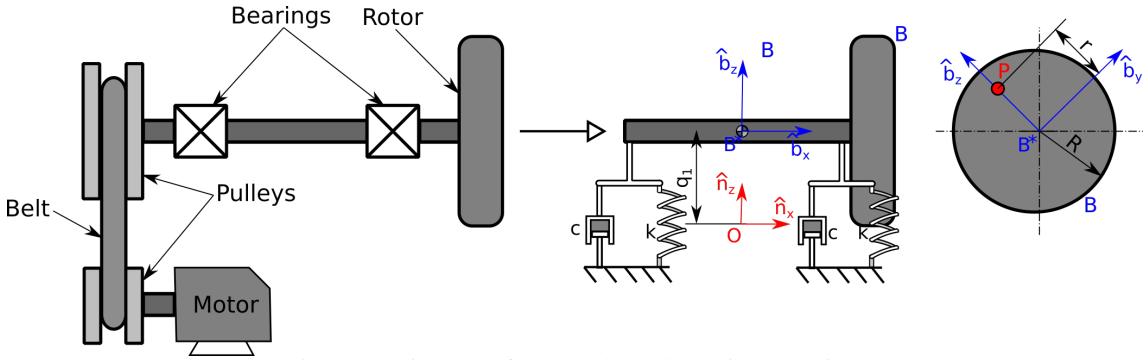

Figure 2: Diagram of an unbalanced rotating machine.

According to Vance *et al.* (2010), from the standpoint of rotor dynamics, the most important characteristics of ball bearings are their high radial stiffness and their very low damping. It is important to consider that if the structure supporting the bearing is soft enough, the ball bearing stiffness becomes irrelevant. Nevertheless, many rotating machines have been built with ball bearings mounted in stiff housings, due either to lack of understanding of benefits of support flexibility or to other special considerations, Vance *et al.* (2010). If N is a Newtonian reference frame, B is a reference frame fixed on the rotor B and O is a fixed point in N, the position vector of the rotor center of mass (point B^*) relative to the point O, the velocity of point B^* in N and acceleration of the point B^* in N, respectively $\mathbf{p}^{B^*}$, $\mathbf{v}^{B^*}$ and $\mathbf{a}^{B^*}$ can be expressed as shown in Eq. (1).

$$\mathbf{p}^{B^*} = q_1\hat{\mathbf{n}}_\mathbf{z}; \qquad \mathbf{v}^{B^*} = u_1\hat{\mathbf{n}}_\mathbf{z}; \qquad \mathbf{a}^{B^*} = \dot{u}_1\hat{\mathbf{n}}_\mathbf{z}; \qquad u_1 = \dot{q}_1 \tag{1}$$

Where the point O coincides with the position of the center of mass when the system is in static equilibrium, q_1 is a generalized coordinate, u_1 is a motion variable, and $\hat{\mathbf{n}}_\mathbf{z}$ is the unit vector related to the z axis of the reference frame N. According to Kane and Levinson (1985), a given mechanical system of n degrees of freedom, the velocity of a point, and the angular velocity of a body with respect to N can be written in a particularly advantageous way by introducing n quantities $u_1, .., u_n$, called motion variables for the system in N. These motion variables can be written as showed in Eq. (2). Where Y_{rs} and Z_r are functions of the generalized coordinates and the time t.

$$u_r = \sum_{s=1}^{n} Y_{rs}\dot{q}_s + Z_r \qquad (r = 1, ..., n) \tag{2}$$

Consider that the rotor rotates at a constant angular speed ω with respect to the Newtonian reference frame N. In this case, the position of the unbalanced mass (point P) relative to the point O, the velocity of P in N and the acceleration of P in N, respectively $\mathbf{p}^P$, $\mathbf{v}^P$ and $\mathbf{a}^P$ can be written as shown in Eq. (3).

$$\mathbf{p}^P = q_1\hat{\mathbf{n}}_\mathbf{z} + r\hat{\mathbf{b}}_\mathbf{z}; \qquad \mathbf{v}^P = u_1\hat{\mathbf{n}}_\mathbf{z} + \omega r\hat{\mathbf{b}}_\mathbf{y}; \qquad \mathbf{a}^P = \dot{u}_1\hat{\mathbf{n}}_\mathbf{z} + \omega^2 r\hat{\mathbf{b}}_\mathbf{z} \tag{3}$$

Where $\hat{\mathbf{b}}_\mathbf{z}$ and $\hat{\mathbf{b}}_\mathbf{y}$ are respectively unit vectors related to the Z and Y axis of the reference frame B. The mechanical system under analysis is composed of a rigid body B (rotor) and a particle P (unbalanced mass) and has one degree of freedom, thus, the system will have two holonomic partial speeds in N, $\mathbf{v}_1^{B^*}$ and $\mathbf{v}_1^P$, as defined by Kane and Levinson (1985). These holonomic partial speeds are shown in Eq. (4).

$$\mathbf{v}_1^{B^*} = \frac{{}^N\partial^N\mathbf{v}^{B^*}}{\partial u_1} = \hat{\mathbf{n}}_\mathbf{z}; \qquad \mathbf{v}_1^P = \frac{{}^N\partial^N\mathbf{v}^P}{\partial u_1} = \hat{\mathbf{n}}_\mathbf{z} \tag{4}$$

According to Kane and Levinson (1985) if S is a holonomic system possessing n degrees of freedom in N, and F_r and F_r^* $(r = 1, ..., n)$ are respectively the holonomic generalized active forces and the holonomic generalized inertia forces for S in N, then Eq. (5) govern all motions of S in any reference frame.

$$F_r + F_r^* = 0 \qquad (r = 1, ..., n) \tag{5}$$

Where in general the generalized active forces acting on the mechanical system S are defined as Eq. (6).

$$F_r = \sum_{i=1}^{\nu} \boldsymbol{v}_r^{P_i} \cdot \boldsymbol{R}_i + {}^{R_1}\boldsymbol{\omega}_r^{R_k} \cdot \boldsymbol{T}_i \quad r = 1, 2, ..., n \tag{6}$$

Where ν is the number of bodies comprising S, R_k is the reference frame fixed in the i^{th} body of S, P_i is a typical particle of the i^{th} body of S, $\boldsymbol{v}_r^{P_i}$ and ${}^{R_1}\boldsymbol{\omega}_r^{R_k}$ are, respectively, the partial velocity and the partial angular velocity of P_i in R_1, and $\boldsymbol{R_i}$ and $\boldsymbol{T_i}$ are, respectively, the resulting of all forces and torques acting on P_i. In a similar way, Kane and Levinson (1985) defined the generalized inertial forces as Eq. (7).

$$F_r^* = \sum_{i=1}^{\nu} \boldsymbol{v}_r^{P_i} \cdot (-m_i \boldsymbol{a_i}) - {}^{R_1}\boldsymbol{\omega}_r^{R_k} \cdot (\boldsymbol{I}_{m_i} \cdot {}^{R_1}\boldsymbol{\alpha}^{R_k} + {}^{R_1}\boldsymbol{\omega}^{R_k} \times \boldsymbol{I}_{m_i} \cdot {}^{R_1}\boldsymbol{\omega}^{R_k}) \quad r = 1, 2, ..., n \tag{7}$$

Where m_i, $\boldsymbol{a_i}$, and $\boldsymbol{I}_{m_i}$ are, respectively, the mass, the acceleration and the inertia of the i^{th} body, and ${}^{R_1}\boldsymbol{\omega}^{R_k}$ and ${}^{R_1}\boldsymbol{\alpha}^{R_k}$ are, respectively, the angular velocity and the angular acceleration of the frame R_k in R_1. The equations of motions are obtained by the sum of Eq. (6) and Eq. (7). According to Liu *et al.* (2005), the form of the equations is quite simple, and calculating Kane equations only engages in additions, subtractions, and multiplications, thereby it is significantly convenient to construct and solve the dynamic equations for complex systems. Furthermore, when using Kane's Method, the task of adding more particles to the system (representing more unbalanced masses) is easy to accomplish.

Back to the system shown in Figure 2, the generalized active force F_1 and the generalized inertia force F_1^* are expressed according to Eq. (8).

$$F_1 = (-2kq_1\hat{\mathbf{n}}_\mathbf{z} - 2cu_1\hat{\mathbf{n}}_\mathbf{z}) \cdot \mathbf{v}_1^{B*}; \qquad F_1^* = -m\,{}^N\mathbf{a}^P \cdot \mathbf{v}_1^P - (M - m)\,{}^N\mathbf{a}^{B*} \cdot \mathbf{v}_1^{B*} \tag{8}$$

Thus, the equation of motion Eq. (9) is obtained.

$$M\dot{u}_1 + 2cu_1 + 2kq_1 = M\ddot{q}_1 + 2c\dot{q}_1 + 2kq_1 = -m\omega^2 r\cos\omega t \tag{9}$$

Note that Eq. (9) is a non-homogeneous second order ODE. Thus, the solution of the system q_1 will be composed of the homogeneous solution q_h (free vibration) added to the particular solution q_p (unbalance response). Furthermore, it is observed that the unbalance generates a harmonic force proportional to the square of the shaft rotation speed. One can consider that the system will respond to this harmonic force with a harmonic behavior as well, but with a slight delay. This delay in response can be counted as a phase angle ϕ and the response amplitude is called Q_D. The particular solution q_P and its time derivatives u_P and $\dot{u}_P$ can be written as shown in Eq. (10).

$$q_P = Q_D\cos(\omega t + \phi) \qquad u_P = -\omega Q_D\sin(\omega t + \phi) \qquad \dot{u}_P = -\omega^2 Q_D\cos(\omega t + \phi) \tag{10}$$

Substituting Eq. (10) into Eq. (9), the magnitude of the amplitude Q_D and the phase angle is derived as can be seen in Eq. (11).

$$|Q_D| = \frac{m\omega^2 r}{\sqrt{(2k - M\omega^2)^2 + (2c\omega)^2}}; \qquad \tan\phi = \frac{2c\omega}{2k - M\omega^2} \tag{11}$$

The unbalance response amplitude (mr) can be derived by dividing the numerator and denominator of the amplitude modulus equation by the total mass of the system M. This operation yields to Eq. (12). This equation is known as the nondimensional amplitude of the response.

$$\frac{MQ_D}{mr} = \frac{\left(\frac{\omega}{\omega_n}\right)^2}{\sqrt{\left(1 - \left(\frac{\omega}{\omega_n}\right)^2\right)^2 + \left(2\zeta\frac{\omega}{\omega_n}\right)^2}} \tag{12}$$

Where the natural frequency ω_n and the damping factor ζ are defined as in Eq. (13).

$$\omega_n = \sqrt{\frac{2k}{M}}; \qquad \zeta = \frac{c}{M\omega_n} \tag{13}$$

It is observed that the maximum value of Eq. (12) occurs when $w = w_n$ and is equal to $1/2\zeta$. According to Vance *et al.* (2010) ball bearings have high radial stiffness and very low damping. That is, at high angular velocities, close to the system's natural frequencies, the response amplitude is very high due to the low damping inherent to these bearings. Figure 3 shows Eq. (12) plotted for different values of the damping factor.

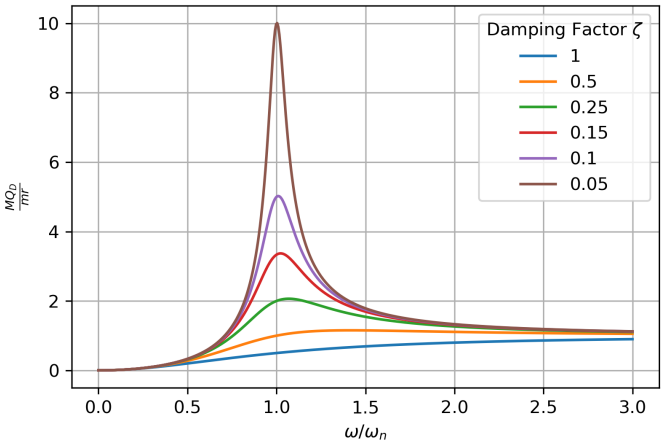

Figure 3: Dynamic Amplification Factor.

3. Case Study, Rotor Test Bench and its Modelling

3.1 Case study:

The case study is a large exhausting fan from the manufacturer GEMA model AF-1635-SE (Figure 4 a) with a flow rate of 30000m³/h and rotation of 750 rpm applied to a multinational company in the tire manufacturing industry. This machine is composed of a 1.5m diameter rotor with a mass of 500kg, a shaft 1.5 meters long and 110mm in diameter, the cantilever rotor is fixed at one end and a pulley at the other end, which is moved by a belt connected to the driving pulley in 175 HP electric motor. The main shaft is supported by two roller bearings (bearing housing SNS 522, roller bearing SKF 22222), located between the rotor and the driven pulley, as shown in Figure 4 a.

The local maintenance team reported two consecutive bearing failures in less than 4 months of operation. Considering the value of bearings, repair labor, and machine downtime, the total cost of this corrective maintenance was more than 50 thousand reais.

Even after the second change of bearings, operators still reported that the machine continued to present high vibration. Vibration analysis was requested to assess the condition of the machine. Through the analysis of the vibration results, the case of unbalance in the exhaust rotor was diagnosed, because the vibration occurred with a dominant peak at the frequency of 1X the rotation of the rotor shaft (750 rpm), greater amplitudes in the horizontal direction, values of unbalance above of 15mm/s peak (the limit according to the ISO21940 Standard would be 6.3mm/s peak).

The balancing service in the loco was performed using a balancing system through the vibration sensor and tachometer, which indicates the need to add a 78g balancing mass at the 70° position in relation to the test mass point Figure 4 b. After balancing, the vibration amplitude of the system reduced from 16.61mm/s to 2.25mm/s (reduction of more than 85% in vibration levels) according to the frequency spectra in Figure 5, each machine operated without new breaks. The evaluation analyzes were carried out with machine operating and the balancing service was carried out in less than two hours of machine downtime, which time was planned with production. This service cost a total of 6 thousand reais, while corrective maintenance performed previously took a total of 23 hours and cost about 50 thousand reais.

3.2 Computational simulation:

Using Kane's method presented in section 2. the rotating system of the case study was modeled in a similar way to the one shown in Figure 2. The equations of motion were generated and simulated using the Python language, using the SymPy library, Gede *et al.* (2013). The rotating system was simulated accordingly to data from the case study and can be

(a) Vibration measurement on exhausting fan.

(b) Balance weight of 78g on the Rotor.

Figure 4: Case study.

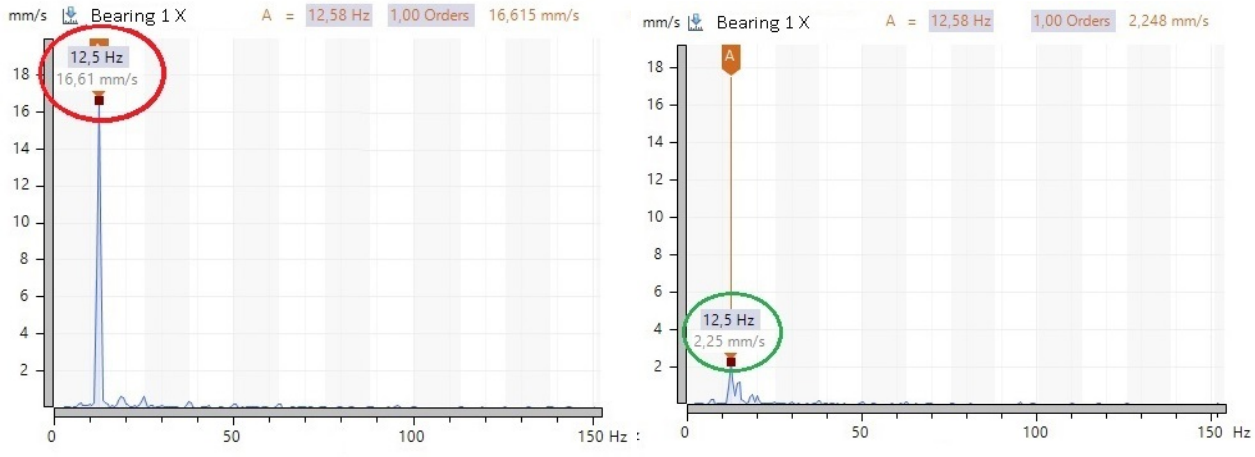

(a) Spectrum before rotor balance.

(b) Spectrum after rotor balance.

Figure 5: Vibration frequency spectrum.

seen in Table 1. The bearing stiffness and damping coefficient were obtained by algebraic manipulation of Eq. (10), Eq. (12), Eq. (13) and considering that the rotor is operating near to the natural frequency deriving to Eq. (14). Table 1 shows the values of the bearing stiffness and damping coefficient obtained using the information shown in Figure 5 and Eq. (14).

$$k = \frac{\omega_n^2 \left(M_e + M_r\right)}{2}; \qquad c = \frac{mr\omega_n}{2Q_D} \tag{14}$$

From the simulation, it was obtained the value of 15.93mm/s for the speed amplitude in the steady-state, corresponding to an error of 4.1% when compared to the study case.

Table 1: Simulation Parameters.

Symbol	Meaning	Value	Symbol	Meaning	Value
M_e	Shaft mass	450kg	R_r	Rotor radius	0.75m
m	Unbalanced mass	0.075kg	r	Unbalanced mass distance	0.75m
$M_r - m$	Rotor mass	500kg	h	Rotor length	0.45m
L	Distance between bearings	0.8m	ω	Angular velocity	78.54 rad/s
L_t	Total shaft length	1.5m	k	Bearing stiffness	2930052.51 N/m
R_e	Shaft radius	0.055m	c	Bearing damping	10514.54 Ns/m

3.3 Experiment:

In the experiments done on the test rig, there were used four different unbalance masses of 0 grams (just residual unbalance around 0g to 1g), 3g, 6g, and 9g. These last three masses were made by weighing M3 bolts with some nuts and washers until achieving the exact weight mentioned. For each mass, the system was initially tested with five different

rotational speeds of 500, 750, 1000, 1250, and 1500 rpm. Vibration readings were taken in the radial direction of bearing 1. The graph in Figure 6 shows the vibration amplitude for global measurements and for the first order peak for all these mentioned tests. Through this graph, it is possible to see the destructive power of unbalance, achieving dangerous vibration amplitude as the rotational speed increases and the excitation frequency approaches the natural frequency of the system. Due to the safety reasons related to the great vibration levels, tests with the unbalance mass of 3g, 6g, and 9g had to be stopped for rotational speeds above 1500 RPM. Global and 1X vibration levels follow the same trending of increase. However, the global levels are slightly higher because they carry vibration information from all frequencies of the vibration reading, which in this case was from 2Hz to 100Hz, while the 1X level is the specific way of unbalance manifest itself in the vibration behavior.

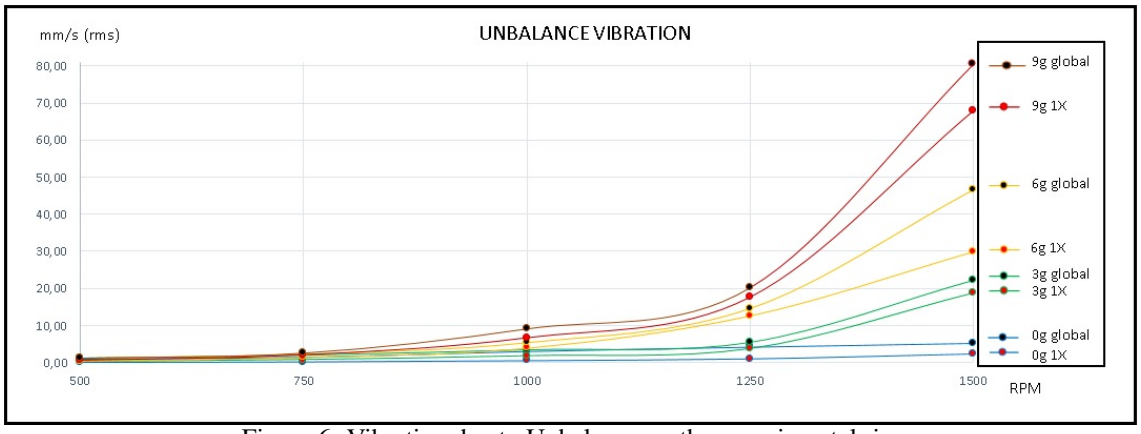

Figure 6: Vibration due to Unbalance on the experimental rig.

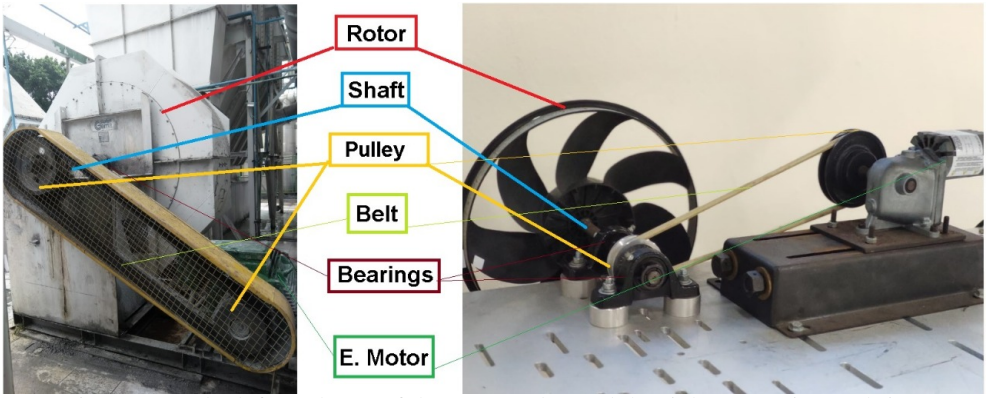

Figure 7: In the left "Exhaust of the case study" and the right "Experimental rig".

As mentioned before, the way used to obtain the stiffness and damping of the case study was assuming that, due to the high difference amplitude from unbalanced to the balanced condition, the system was operating near to the natural frequency, where the dynamic amplification influence is more relevant. So, for results of the experimental test rig, a bump test was done to evaluate the natural frequency of the system. For the results of the tests presented in Figure 6 the bump tests done show a natural frequency of 39,3Hz, as shown in Figure 8. After the first tests, it was observed that some adjustments, such as tightening bolts and stretching the belt, influence a lot on the system stiffness, consequently changing the natural frequency. Just with belt stretch and better bearing block bolts tightened, the natural frequency of the system changes from 39,3Hz to 46Hz.

For the simulation model, there were considered some simplifications and considerations, where one of them was that one plane unbalance vibrations occurs in phase between bearings 1 and 2. To check and prove it, a special measurement was done on the test rig using two accelerometers (channel 1 and Channel 2), one for each bearing, positioned in the same radial direction and measuring the vibration at the exact same time. The result of this reading shows that in the 1st order frequency, both bearings vibrates in phase as shown in the Figure 9. Just a small difference of 3° of phase was found. That bellow 10° can be considered in phase.

Due to the safety reasons related to the great vibration levels, tests with rotation frequency higher than the natural frequency were performed just for the residual unbalanced condition 0g. The maximum frequency of tests was around 60Hz due to the used electrical motor limit of 3590 RPM. To operate at this maximum rotational speed it was necessary to do some belt stretching tighten (slack belt rotating at high speed, generated high vibration at frequencies not related to

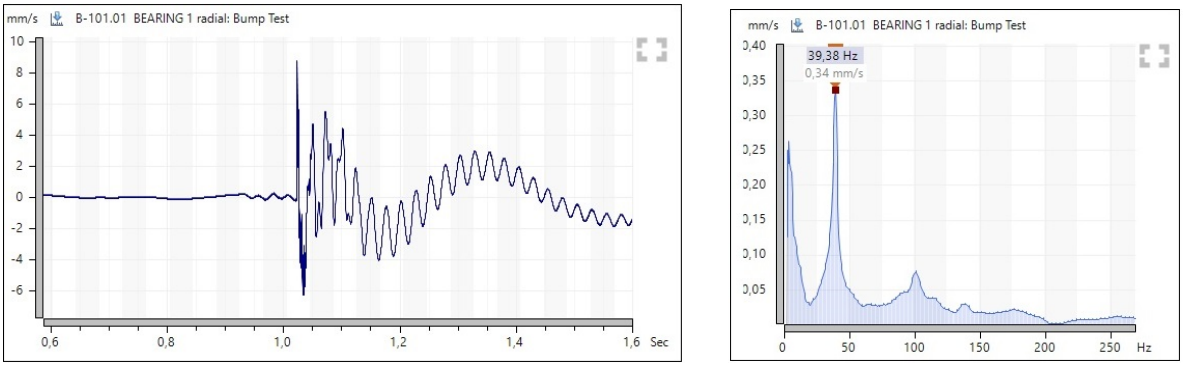

(a) Time signal. (b) Spectrum spectrum.

Figure 8: Bump test for natural frequency evaluation.

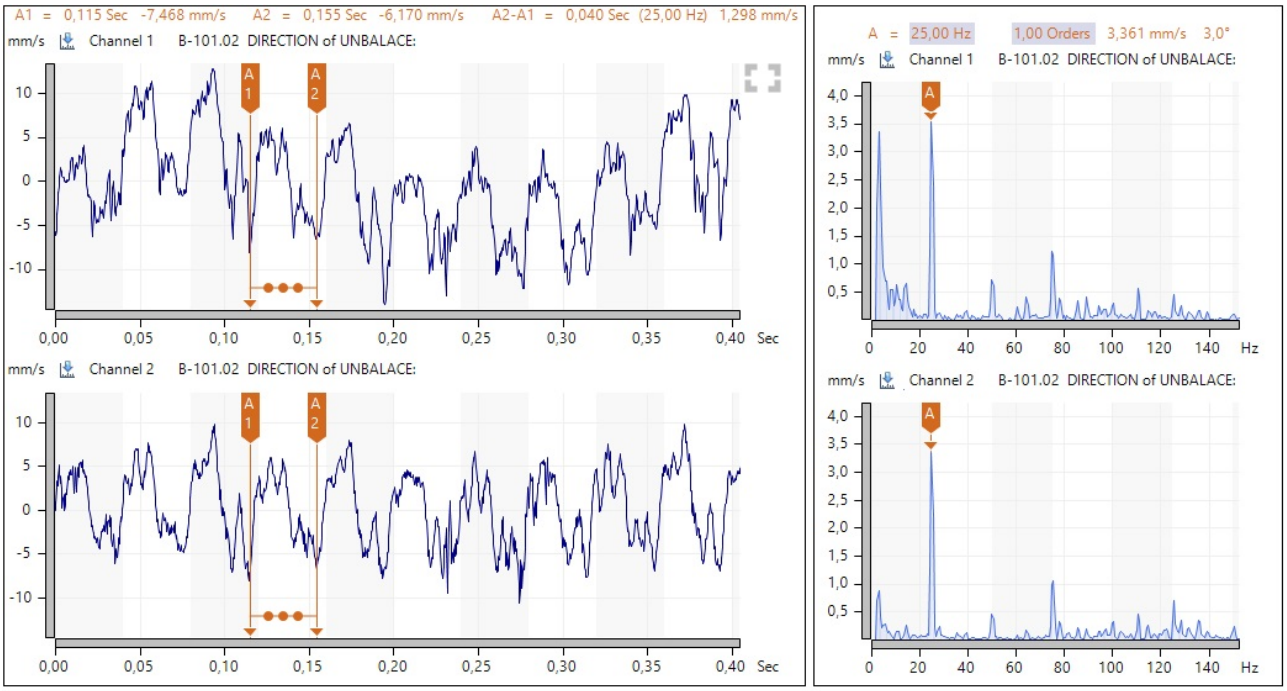

Figure 9: In phase vibration measurements between bearing 1 and 2.

unbalance, hindering the experiment), changing the stiffness of the system and the natural frequency from 39hz to 46Hz. In this way, a maximum of just 1,3X from the natural frequency was possible to be achieved in the experiments. The Tab. 2 shown the 1X frequency vibration amplitude results for the experiments, and simulation. Comparing simulation results to the experiments it is noted that simulation works better for the frequencies from 0,65 to 1,3 times of the natural frequency(25,0Hz to 59,8Hz), with a medium error of 14,4%. To the low frequencies, below 0,65 of natural frequency (8,3 Hz to 20,8 Hz), the simulation results are not satisfactory, with a medium error of 79,3%. However, according to the dynamic amplification graph, Figure 3, the most important frequency region is exactly the one around 0,6 to 1,4 of the natural frequency, where the simulation results are with better converging levels. This converging level of simulation results related to the experimental tests performed is a great indication of the confirmation that the case study was operating near the natural frequency.

4. CONCLUSIONS

Through the results presented in this paper and the relation between the case study, simulation, and the experiment done, it can be concluded that in the case study beyond the unbalancing condition the system operates near to the natural frequency, even though this condition was not measured in the real case. By the experiments performed on this work, it was clearly observed the direct relation of unbalanced condition to the 1st order frequency on the vibration levels, where it is more sensitive to the radial direction of measurements. The simulation model done works better for frequencies up to 30% of the natural frequency of the system, the region where the unbalance condition has more influence due to the dynamic amplification. However, the 1DOF model may not be suitable for the cantilever rotor case. Unbalance

Table 2: 1X Vibration (mm/s rms) to Frequencies from 8.3Hz to 59.8Hz.

Mass	Result	8.3	12.5	16.7	20.8	25.0	39.3	42.3	44.9	46.0	55.1	59.8
0g	Exp.	0.02	0.14	0.45	0.89	2.14	19.96	21.60	22.10	26.30	32.85	37.90
0g	Sim.	0.41	1.28	2.76	4.70	5.77	16.32	17.73	19.04	26.40	34.96	37.91
3g	Exp.	0.19	0.70	1.73	3.68	18.80	46.19	-	-	-	-	-
3g	Sim.	1.23	3.86	8.35	14.09	20.10	46.45	53.20	57.13	63.20	78.33	97.44
6g	Exp.	0.37	7.72	3.88	12.57	29.83	-	-	-	-	-	-
6g	Sim.	2.46	7.72	16.70	28.18	40.20	91.82	106.40	114.26	108.82	156.65	194.88
9g	Exp.	0.50	1.96	6.58	17.55	67.85	-	-	-	-	-	-
9g	Sim.	3.70	11.58	25.05	42.27	63.82	139.35	159.60	171.40	163.24	234.97	292.31

conditions can be better controlled, in terms of vibration behavior, when the excitation frequency is far from natural frequency. So, it is very important to keep in control all parameters that can change system stiffness as belt stretch and foundation bolts tighten on the bearing blocks. Because changes on these parameters will cause considerable changes in the stiffness and, consequently, variations on the system natural frequency which can lead to an inappropriate region of operational frequencies, where the vibration behavior can be dynamic amplified in high levels. For the real case of unbalanced machines, it is suggested to carry out a response test to evaluate the natural frequencies of the system related to the unbalance excitation frequency, which must be at least 40% distant from each other to operate in a "vibration zone of security". The destructive power of unbalance was shown through the Figure 6 where the tests had to be stopped for the unbalanced condition for the rotation speeds above 1500 rpm due to the dangerous vibration amplitude levels as the rotational speed increases and the excitation frequency approaches the natural frequency of the system. For further experiments, it will be considered to use a heavier rotor and higher length cantilever shaft to reduce the system natural frequency and then be able to evaluate a better region of frequencies above the natural frequency, where is expected to see a decrease of vibration levels when achieving frequencies above 1,4X of the natural frequency.

5. REFERENCES

AHRI, 2019. *Guideline for Mechanical Balance of Impellers for Fans - Mechanical Vibration – Mechanical vibration – Rotor balancing*. ISO Standard 21940-21:2019, - Part 21: Description and evaluation of balancing machines, 2019, International Organization for Standardization, Case Postale 56, CH-1211, Geneva 21 Switzerland, 2019.

Ambur, R. and Rinderknecht, S., 2018. "Unbalance detection in rotor systems with active bearings using self-sensing piezoelectric actuators". *Mechanical Systems and Signal Processing*, Vol. 102, pp. 72–86.

Braga, D., 2019. *Desalinhamento de eixos em Máquinas*. Celulose Online, https://www.celuloseonline.com.br/artigo-tecnico-desalinhemento-de-eixos-em-maquinas/ Acesso em 28/04/2021.

Gede, G., Peterson, D.L., Nanjangud, A.S., Moore, J.K. and Hubbard, M., 2013. "Constrained multibody dynamics with python: From symbolic equation generation to publication". In *International Design Engineering Technical Conferences and Computers and Information in Engineering Conference*. American Society of Mechanical Engineers, Vol. 55973, p. V07BT10A051.

Kane, T.R. and Levinson, D.A., 1985. *Dynamics, theory and applications*. McGraw Hill.

Levitt, J., 2021. "Form a different angle: A perspective - defects, p-f and the rest of story". Accessed: 2020-06-09.

Li, Z., Zheng, T., Wang, Y., Cao, Z., Guo, Z. and Fu, H., 2020. "A novel method for imbalanced fault diagnosis of rotating machinery based on generative adversarial networks". *IEEE Transactions on Instrumentation and Measurement*, Vol. 70, pp. 1–17.

Liu, W.F., Gong, Z.B. and Hong, Q.Q., 2005. "Investigation on kane dynamic equations based on screw theory for openchain manipui. ators". *Applied Mathematics and Mechanics*, Vol. 26, No. 5, pp. 627–635.

Mobius, 2005. *Livro para o Curso de Análise de Vibração*. SEMEQ - Inteligência em Saúde de Máquinas - 2005.

Muszynska, A., 2005. *Rotordynamics*. CRC press.

Rao, S.S., 2009. *Vibrações mecânicas* . Pearson Educación.

Vance, J.M., Zeidan, F.Y. and Murphy, B.G., 2010. *Machinery vibration and rotordynamics*. John Wiley & Sons.

6. RESPONSIBILITY NOTICE

The authors are solely responsible for the printed material included in this paper.